Earth and Planetary Science Letters 427 (2015) 191–201

Contents lists available at ScienceDirect

Earth and Planetary Science Letters

www.elsevier.com/locate/epsl

Composition of the core from gallium metal–silicate partitioning experiments

I. Blanchard [a,*], J. Badro [a,b], J. Siebert [a], F.J. Ryerson [c,a]

[a] Institut de Physique du Globe de Paris, Sorbonne Paris Cité, Université Paris Diderot, CNRS, F-75005 Paris, France
[b] Earth and Planetary Science Laboratory, École Polytechnique Fédérale de Lausanne, CH-1015 Lausanne, Switzerland
[c] Lawrence Livermore National Laboratory, Livermore, CA 94551, USA

ARTICLE INFO

Article history:
Received 29 November 2014
Received in revised form 27 June 2015
Accepted 29 June 2015
Available online 24 July 2015
Editor: J. Brodholt

Keywords:
gallium partitioning
light elements
accretion and differentiation of the Earth
deep magma ocean

ABSTRACT

Gallium concentration (normalized to CI chondrites) in the mantle is at the same level as that of lithophile elements with similar volatility, implying that there must be little to no gallium in Earth's core. Metal-silicate partitioning experiments, however, have shown that gallium is a moderately siderophile element and should be therefore depleted in the mantle by core formation. Moreover, gallium concentrations in the mantle (4 ppm) are too high to be only brought by the late veneer; and neither pressure, nor temperature, nor silicate composition has a large enough effect on gallium partitioning to make it lithophile. We therefore systematically investigated the effect of core composition (light element content) on the partitioning of gallium by carrying out metal–silicate partitioning experiments in a piston–cylinder press at 2 GPa between 1673 K and 2073 K. Four light elements (Si, O, S, C) were considered, and their effect was found to be sufficiently strong to make gallium lithophile. The partitioning of gallium was then modeled and parameterized as a function of pressure, temperature, redox and core composition. A continuous core formation model was used to track the evolution of gallium partitioning during core formation, for various magma ocean depths, geotherms, core light element contents, and magma ocean composition (redox) during accretion. The only model for which the final gallium concentration in the silicate Earth matched the observed value is the one involving a light-element rich core equilibrating in a FeO-rich deep magma ocean (>1300 km) with a final pressure of at least 50 GPa. More specifically, the incorporation of S and C in the core provided successful models only for concentrations that lie far beyond their allowable cosmochemical or geophysical limits, whereas realistic O and Si amounts (less than 5 wt.%) in the core provided successful models for magma oceans deeper that 1300 km. These results offer a strong argument for an O- and Si-rich core, formed in a deep terrestrial magma ocean, along with oxidizing conditions.

1. Introduction

The segregation of the Earth's crust, mantle and core are the primary geochemical differentiation events in the evolution of the planet, and their cumulative impact is recorded in the compositions of these reservoirs. Core formation occurred early in Earth history and the effects of this metal–silicate interaction can be observed in the mantle's siderophile element abundance patterns in which these elements are depleted relative to their concentrations in meteorites (Ringwood, 1966). Similarly, seismic observations requiring incorporation of light elements in the core (Birch, 1952, 1964) may also be a product of metal–silicate equilibration.

Numerous models of planetary accretion and core formation have been proposed, invoking single-stage and continuous core formation models over a range of P–T–fO_2 conditions (e.g. Thibault and Walter, 1995; Li and Agee, 1996; Righter et al., 1997; Gessmann and Rubie, 2000; Chabot and Agee, 2003; Chabot et al., 2005; Wade and Wood, 2005; Corgne et al., 2008; Corgne et al., 2009; Mann et al., 2009; Cottrell et al., 2009; Siebert et al., 2011). These scenarios couple the geochemical evolution of the core and mantle. Ideally, successful models must reproduce both the siderophile element patterns in the silicate mantle and provide the necessary complement of light elements to the core required to reconcile its density deficit relative to iron. Many core–mantle segregation models are capable of reproducing mantle abundance patterns for moderately siderophile elements (Gessmann and Rubie, 2000; Chabot and Agee, 2003; Wood et al., 2009; Siebert et al., 2011; Siebert et al., 2012), but

* Corresponding author.
E-mail address: blanchard@ipgp.fr (I. Blanchard).

http://dx.doi.org/10.1016/j.epsl.2015.06.063
0012-821X/

the addition of a late veneer is required to match the mantle concentrations of the highly siderophile elements, indicating that core–mantle segregation alone may not fully describe the evolution of these reservoirs (Ertel et al., 1996; Holzheid et al., 2000; Brenan and McDonough, 2009). In addition, dynamical models of the late-stage accretion of the Earth, invoking large impacts of various size and trajectory, often posit direct physical coalescence of the proto-Earth core with that of the impactor (Rubie et al., 2011). This again may decouple the compositional evolution of the core and mantle. Nevertheless, single-stage and continuous core formation models provide a point of departure for consideration of the geochemical consequences of such events, with metal–silicate partitioning obtained over an appropriate range of P–T–fO_2 conditions specifying the required geochemical constraints.

The partitioning of siderophile elements is typically characterized as a K_D,

$$K_D^m = \frac{[m_{metal}][\mathrm{Fe}_{silicate}]^{n/2}}{[m_{silicate}][\mathrm{Fe}_{metal}]^{n/2}} \quad (1)$$

that quantifies the exchange of an element, m with a valence n, and Fe between the silicate and Fe-metal phase; and has been studied by many investigators leading to parameterizations for numerous siderophile elements as a function of P–T–fO_2–X conditions (Li and Agee, 1996; Wade and Wood, 2005; Corgne et al., 2008; Mann et al., 2009; Siebert et al., 2011). The Fe concentration of the mantle is a direct consequence of the oxygen fugacity evolution of the mantle ($\mathrm{Fe}_{metal} + 1/2\mathrm{O}_2 = \mathrm{FeO}_{silicate}$) and agreement with the current FeO concentration of the mantle provides an additional constraint on core formation models. The influence of oxygen fugacity on siderophile partitioning is widely appreciated. For instance, Wood et al. (2006) have proposed a continuous core formation model in which an initially reduced mantle is progressively oxidized during accretion, successfully capturing the mantle concentrations for numerous moderately siderophile elements. Another, more recently appreciated, factor is the influence of light element solubility in the metallic core-forming liquid on the activity coefficients of moderately siderophile elements in that liquid alloy (Wade and Wood, 2005; Corgne et al., 2009; Siebert et al., 2011). Corgne et al. (2009), using the interaction parameter approach and thermodynamic data from the metallurgical literature, estimated the influence of light element solubility on siderophile element activity coefficients and metal–silicate partitioning, and were able to reconcile the mantle concentrations of moderately siderophile elements by single-stage core formation around IW-2. More recently, LH-DAC experiments at pressures and temperatures directly relevant to metal–silicate equilibration at the base of a deep magma ocean (about 1300 km) verified incorporation of oxygen in the metallic phase at relatively high concentrations (up to 5.5 wt.%) and demonstrated its influence on siderophile element partitioning (Siebert et al., 2013).

Here, we investigate the effect of light elements (silicon, oxygen, sulfur and carbon) dissolved in the core-forming metallic liquid on the partitioning of gallium between metal and silicate. The concentration of gallium in the Earth's mantle (4 ppm) has been determined from ultramafic xenoliths (O'Neill and Palme, 1998). Gallium is a moderately siderophile element found in abundance in the metal phase of iron meteorites (Scott and Wasson, 1975). Despite its siderophile character, gallium in the Earth's mantle plots directly on the volatility trend of lithophile elements (McDonough, 2003) suggesting that it was not depleted by core formation.

Most of previous works on gallium metal–silicate partitioning by Corgne et al. (2008), Mann et al. (2009) and Siebert et al. (2011) failed to account for the excess of Ga in the silicate Earth by core–mantle equilibration at high pressure and high temperature. Righter and Drake (2000) and Righter (2011) showed that required D_{Ga} of the Earth could be accounted by core–mantle equilibration (at 30 GPa and 3230 °C), but at an oxygen fugacity of IW-1 not consistent with the present FeO content of the mantle. Also, unlike the highly siderophile elements (Au, Re, PGEs), gallium concentrations cannot be reconciled by invoking the addition of a late veneer (McDonough and Sun, 1995; Palme and O'Neill, 2003; Brenan and McDonough, 2009) as gallium concentration of the mantle would require a late veneer equivalent to ~20% of the Earth's mass, while highly siderophile element concentrations require only 0.5% after core formation (Brenan and McDonough, 2009; Siebert et al., 2011).

Here, we specifically consider the influence of light element solubility on gallium partitioning as a potential solution to this paradox. We investigated systematically the effect of light elements dissolved in metal on gallium partitioning between metal and silicate at low pressure and low temperature using an end load piston–cylinder apparatus. Following many previous studies (i.e. Gessmann et al., 2001; Wade and Wood, 2005; Chabot et al., 2003; Mann et al., 2009; Siebert et al., 2011), our results have then been extrapolated at pressure and temperature relevant to core formation using a continuous core formation model to assess the influence of light elements trapped in the core on Ga partitioning. Those models include four realistic redox paths (from reduced to oxidized) that have been proposed in the literature to obtain a relevant partitioning of Ga between metal and silicate. Those simulations highlight the important effect of incorporating light elements into the metallic phase to decrease gallium partitioning, and illustrate that only scenarios of oxidizing conditions during Earth differentiation permit to reproduce gallium behavior on Earth, along with high pressure of equilibration.

2. Metal-silicate partitioning

Gallium partitioning between metal and silicate can be written as a chemical exchange (redox) reaction:

$$\frac{3}{2}\mathrm{Fe}^{metal} + \mathrm{GaO}_{3/2}^{silicate} = \mathrm{Ga}^{metal} + \frac{3}{2}\mathrm{FeO}^{silicate} \quad (2)$$

where gallium has a valence of 3+ (Drake et al., 1984; Schmitt et al., 1989; Capobianco et al., 1999; Jaeger and Drake, 2000; Righter and Drake, 2000; Righter, 2011; Righter et al., 2010) and iron 2+.

The metal–silicate partition coefficient is the molar concentration ratio:

$$D_{\mathrm{Ga}} = \frac{X_{\mathrm{Ga}}^{metal}}{X_{\mathrm{GaO}_{3/2}}^{silicate}} \quad (3)$$

The equilibrium constant associated with reaction (2) is:

$$K = \frac{(a_{\mathrm{FeO}}^{silicate})^{\frac{3}{2}}(a_{\mathrm{Ga}}^{metal})}{(a_{\mathrm{GaO}_{\frac{3}{2}}}^{silicate})(a_{\mathrm{Fe}}^{metal})^{3/2}} \quad (4)$$

In equation (4), a is the activity of the different components, so that $a_i = \gamma_i X_i$, where γ_i is the activity coefficient and X_i the mole fraction. Hereafter, we are using the approach proposed by Wade and Wood (2005) and used extensively in the literature (i.e. Corgne et al., 2008, 2009; Wood et al., 2009; Ricolleau et al., 2011; Siebert et al., 2011) to parameterize the equilibrium constant.

Taking logarithm of equation (4) yields:

$$\log K = \log \frac{X_{\mathrm{Ga}}^{metal}(X_{\mathrm{FeO}}^{silicate})^{3/2}}{X_{\mathrm{GaO}_{\frac{3}{2}}}^{silicate}(X_{\mathrm{Fe}}^{metal})^{3/2}} + \log \frac{\gamma_{\mathrm{Ga}}^{metal}}{(\gamma_{\mathrm{Fe}}^{metal})^{3/2}} + \log \frac{(\gamma_{\mathrm{FeO}}^{silicate})^{3/2}}{\gamma_{\mathrm{GaO}_{\frac{3}{2}}}^{silicate}} \quad (5)$$

Siebert et al. (2011) showed that Ga metal–silicate partitioning is not influenced by silicate melt composition. Thus, in the following, we consider $\gamma^{silicate}_{GaO_{\frac{3}{2}}}$ to $\gamma^{silicate}_{FeO}$ ratio constant over our range of composition, which leads to:

$$\log K = \log \frac{X^{metal}_{Ga}(X^{silicate}_{FeO})^{3/2}}{X^{silicate}_{GaO_{\frac{3}{2}}}(X^{metal}_{Fe})^{3/2}} + \log \frac{\gamma^{metal}_{Ga}}{(\gamma^{metal}_{Fe})^{3/2}} \quad (6)$$

Equation (6) can be rewritten as:

$$\log K = \log K_D + \log \frac{\gamma^{metal}_{Ga}}{(\gamma^{metal}_{Fe})^{3/2}} \quad (7)$$

with K_D the exchange coefficient measured experimentally.

Values of activity coefficient γ^{metal}_{Ga} and γ^{metal}_{Fe} were calculated using the interaction parameter approach presented in Ma (2001) that is consistent and obey the Gibbs–Duhem equation. This method use tabulated interaction parameters ε from The Japan Society for the Promotion of Science and The Nineteenth Committee on Steelmaking (1988). The interaction parameters ε^j_i reflects the measured effects of a component (j) on the activity of another one (i) in an iron alloy and allows us to correct our partitioning for solute interaction. The activity coefficient of iron and the $N-1$ solutes (i) in a metallic solution containing N components is expressed as:

$$\begin{aligned}\ln \gamma_{Fe} = {} & \sum_{i=1}^{N-1} \varepsilon^i_i\left(X_i + \ln(1-X_i)\right) \\ & - \sum_{j=1}^{N-2}\sum_{k=j+1}^{N-1} \varepsilon^k_j X_j X_k\left(1 + \frac{\ln(1-X_j)}{X_j} + \frac{\ln(1-X_k)}{X_k}\right) \\ & + \sum_{i=1}^{N-1}\sum_{k=1(k\neq i)}^{N-1} \varepsilon^k_i X_i X_k\left(1 + \frac{\ln(1-X_k)}{X_k} - \frac{1}{1-X_i}\right) \\ & + \frac{1}{2}\sum_{j=1}^{N-2}\sum_{k=j+1}^{N-1} \varepsilon^k_j X^2_j X^2_k\left(\frac{1}{1-X_j} + \frac{1}{1-X_k} - 1\right) \\ & - \sum_{i=1}^{N-1}\sum_{k=1(k\neq i)}^{N-1} \varepsilon^k_i X^2_i X^2_k\left(\frac{1}{1-X_i} + \frac{1}{1-X_k}\right. \\ & \left. + \frac{X_i}{2(1-X_i)^2} - 1\right) \end{aligned} \quad (8)$$

and

$$\begin{aligned}\ln \gamma_i = {} & \ln \gamma_{Fe} + \ln \gamma^0_i - \varepsilon^i_i \ln(1-X_i) \\ & - \sum_{j=1(j\neq i)}^{N-1} \varepsilon^j_i X_j\left(1 + \frac{\ln(1-X_j)}{X_j} - \frac{1}{1-X_i}\right) \\ & + \sum_{j=1(j\neq i)}^{N-1} \varepsilon^j_i X^2_j X_i\left(\frac{1}{1-X_i} + \frac{1}{1-X_j} + \frac{X_i}{2(1-X_i)^2} - 1\right) \end{aligned} \quad (9)$$

Values of ε^j_i reported hereafter are at the reference temperature of 1873 K and extrapolated to run temperature following the approach proposed in the Steelmaking Data Sourcebook (The Japan Society for the Promotion of Science and The Nineteenth Committee on Steelmaking, 1988):

$$\varepsilon^{LE}_{Ga}(T) = \frac{T^0}{T}\varepsilon^{LE}_{Ga}(T^0) \quad (10)$$

where T^0 is the temperature at which the tabulated values applied and T the temperature of interest.

3. Experimental procedures

Metal-silicate partitioning experiments were performed in a 150-tons end-loaded piston–cylinder apparatus at 2 GPa and temperatures ranging between 1673 K and 2073 K. We used a 1/2″ piston–cylinder vessel and $BaCO_3$ pressure cells with a graphite furnace and MgO capsule (see Siebert et al., 2011 for further description of the assembly). The assembly was wrapped in a thin lead foil to reduce friction loss and ensure easier extraction after quench. Temperature was measured and regulated using a type-D thermocouple ($W_{97}Re_3/W_{75}Re_{25}$) contained in a 4-hole alumina ceramic sleeve and inserted axially above the capsule. Uncertainties for pressure and temperature are estimated to be around 0.1 GPa and 50 K respectively (Siebert et al., 2011). At conditions of the present experiments both the silicate and the metallic phases were fully molten.

Starting silicate material consists of a natural MORB glass from mid-Atlantic ridge, finely ground and doped with high purity gallium oxide (Alfa Aesar puratronic©). Concentrations of Ga_2O_3 varied from 2 wt.% to 5 wt.% for S-rich and Si-rich metallic compounds, respectively (see below and Table 1).

Three different metal compositions were used in the experiments to systematically investigate the effect of sulfur, silicon and oxygen on the partitioning of gallium: sulfur-bearing runs contained a mixture of Fe + FeS (from 4.1 to 28 wt.% of S in the metallic phase of recovered samples); silicon-bearing runs contained a mixture of Fe + FeSi (from 1.38 to 16.39 wt.% of Si in the metallic phase of recovered samples) and finally Fe + FeS was mixed with FeSi to vary the redox conditions during the experiment, and, in turn, the amount of oxygen dissolved in the metallic (Table 1). The quantity of oxygen in the metallic phase of the recovered run varied from 0.6 to 3.9 wt.%. Experiments at lower temperatures (1673 K) allowed us to separate the effect of sulfur from that of oxygen on the partitioning of gallium (see Sections 5 and 6 for details). Metal and silicate were mixed in a 1:3 ratio to produce the final starting materials. All the powders were finely ground under ethanol in an agate mortar to ensure homogeneity before loading in the MgO capsules.

For high temperature experiments (2073 K), run durations were typically ~ 1 min, which is sufficient to reach chemical equilibrium and minimize the reaction of the silicate melt with the MgO capsule (Thibault and Walter, 1995; Corgne et al., 2008). Experiments conducted at 1673 K were typically ~10 min in duration to ensure chemical equilibration. See Section 4 for further discussion of equilibrium. The samples were quickly quenched by switching off the electric power and then slowly decompressed.

4. Analytical procedures

Recovered samples were mounted in epoxy, polished to 1 micrometer with diamond paste, and carbon coated for SEM and electron probe analysis. Electron microprobe analyses were performed on a JEOL JEM 9210 at LLNL and on a CAMECA SX-five or SX-100 at IPGP (service Camparis, Université Paris 6/IPGP) using an accelerating voltage of 15 keV and a beam current of 10 nA for major elements and 300 nA for gallium (in both silicate and metallic phase) and oxygen (in metallic phase). We used such a high current to improve counting statistics and obtain a better resolution on Ga and O measurements. Detection limit for Ga has thus been lowered to 40 ppm in the silicate phase. As both silicate and metallic melts quenched to heterogeneous assemblages of quench crystals, we used a raster box of 50 microns in the silicate phase

Table 1
Experimental conditions.

Run #	T (K)	P (GPa)	t (min)	Silicate composition	Metal composition	IW[a]
MORB Fe	2073	2	1	MORB + 2 wt.% Ga	100% Fe	−2.46
MORB FeS1	2073	2	1	MORB + 2 wt.% Ga	83 wt.% Fe + 17 wt.% FeS	−2.2
MORB FeS2	2073	2	1	MORB + 2 wt.% Ga	75 wt.% Fe + 25 wt.% FeS	−2.1
MORB FeS3	2073	2	1	MORB + 2 wt.% Ga	80 wt.% Fe + 20 wt.% FeS	−2.2
MORB FeS4	2073	2	1	MORB + 2 wt.% Ga	90 wt.% Fe + 10 wt.% FeS	−1.9
MORB FeS5	2073	2	1	MORB + 2 wt.% Ga	50 wt.% Fe + 50 wt.% FeS	−1.6
MORB Fes7	2073	2	1	MORB + 2 wt.% Ga	25 wt.% Fe + 75 wt.% FeS	−1.9
MORB FeS8	2073	2	1	MORB + 2 wt.% Ga	70 wt.% Fe + 30 wt.% FeS	−1.8
MORB FeS9	2073	2	1	MORB + 2 wt.% Ga	65 wt.% Fe + 35 wt.% FeS	−1.8
MORB FeS10	2073	2	1	MORB + 2 wt.% Ga	60 wt.% Fe + 40 wt.% FeS	−1.8
MORB FeS11	2073	2	1	MORB + 2 wt.% Ga	80 wt.% Fe + 20 wt.% FeS	−2.1
MORB FeS12	2073	2	1	MORB + 2 wt.% Ga	73 wt.% Fe + 27 wt.% FeS	−2.1
MORB FeS13	2073	2	1	MORB + 2 wt.% Ga	70 wt.% Fe +30 wt.% FeS	−2
MORB FeS14	2073	2	1	MORB + 2 wt.% Ga	65 wt.% Fe + 35 wt.% FeS	−1.9
MORB FeSSi5	2073	2	1	MORB + 5 wt.% Ga	57 wt.% Fe + 31 wt.% FeS + 12 wt.% FeSi	−2.4
MORB FeSSi6	2073	2	1	MORB + 5 wt.% Ga	53 wt.% Fe + 29 wt.% FeS + 18 wt.% FeSi	−3.2
MORB FeSSi10	2073	2	1	MORB + 5 wt.% Ga	45 wt.% Fe + 37 wt.% FeS + 18 wt.% FeSi	−3
MORB FeSSi11	2073	2	1	MORB + 5 wt.% Ga	29 wt.% Fe + 53 wt.% FeS + 18 wt.% FeSi	−2.7
MORB Fe5 wt.%	2073	2	1	MORB + 5 wt.% Ga	100 wt.% Fe	−2.2
MORB FeSi70	2073	2	1	MORB + 5 wt.% Ga	70 wt.% Fe + 30 wt.% FeSi	−5.8
MORB FeSi80	2073	2	1	MORB + 5 wt.% Ga	80 wt.% Fe + 20 wt.% FeSi	−5.1
MORB FeSi85	2073	2	1	MORB + 5 wt.% Ga	85 wt.% Fe + 15 wt.% FeSi	−4.9
MORB FeSi90	2073	2	1	MORB + 5 wt.% Ga	90 wt.% Fe + 10 wt.% FeSi	−4.4
MORB FeSi95	2073	2	1	MORB + 5 wt.% Ga	95 wt.% Fe + 5 wt.% FeSi	−3.1
HP-BT 1	1673	2	10	MORB + 2 wt.% Ga	90 wt.% Fe + 10 wt.% FeS	−1.9
HP-BT 2	1673	2	10	MORB + 2 wt.% Ga	80 wt.% Fe + 20 wt.% FeS	−1.8
HP-BT 3	1673	2	10	MORB + 2 wt.% Ga	70 wt.% Fe + 30 wt.% FeS	−1.7
HP-BT 4	1673	2	10	MORB + 2 wt.% Ga	50 wt.% Fe + 50 wt.% FeS	−1.5
HP-BT 5	1673	2	10	MORB + 2 wt.% Ga	40 wt.% Fe + 60 wt.% FeS	−1.5

[a] Oxygen fugacity relative to the iron–wüstite buffer calculated assuming ideal mixing behavior (i.e. $IW = 2 * \log(X_{FeO}/X_{Fe})$.

and 100 microns in the metallic phase, to integrate the composition of the quenched regions. Standards used in these analyses are diopside for SiO_2, MgO, CaO; orthopyroxene for K_2O and Al_2O_3; Fe_2O_3 for iron oxide; albite for Na_2O; FeS_2 for S in the silicate and an alloy of Mn and Ti for TiO_2. For the metallic phase, Fe_2O_3 was used for Fe and O, FeS_2 for sulfur, diopside for Si. For both metal and silicate, gallium arsenide was used as a standard for Ga. Compositions of silicate and metallic phases are given in Tables S1 and S2 in supplementary materials, respectively.

We performed transects in all our samples both in metallic and silicate phase. No compositional zoning was observed either in samples equilibrated at 1673 K during ten minutes, or 2073 K during one minute. This strongly supports that equilibrium was reached in the experiments. It is also consistent with previous studies (e.g. Thibault and Walter, 1995; Corgne et al., 2008), which performed time series experiments at superliquidus conditions similar to those of our work and demonstrated attainment of equilibrium after few tens of seconds.

5. Experimental results

The samples consist of quench blebs of molten alloy surrounded by quenched silicate melt (see Fig. 1 for a typical run product at 2073 K). The nature of the quench assemblage varies with run temperature and composition. At the highest temperatures, dissolution of MgO capsule material in the sample enriched the basalt in MgO resulting in more pyrolitic composition that did not quench to glass. Lesser MgO dissolution in samples synthesized at 1673 K resulted in a homogeneous silicate glass on quench explaining the low standard deviation of theses EPMA analyses (Table S1). The S-rich metallic phase show dendritic textures. At higher S concentrations oxygen-containing blobs are observed in the metallic phase indicative of enhance oxygen solubility in metal for these compositions (see Fig. 3). Such features in metallic phase have been observed previously in the literature (e.g. O'Neill et al., 1998; Gessmann and Rubie, 1998; Chabot et al., 2003 and Mann et al., 2009).

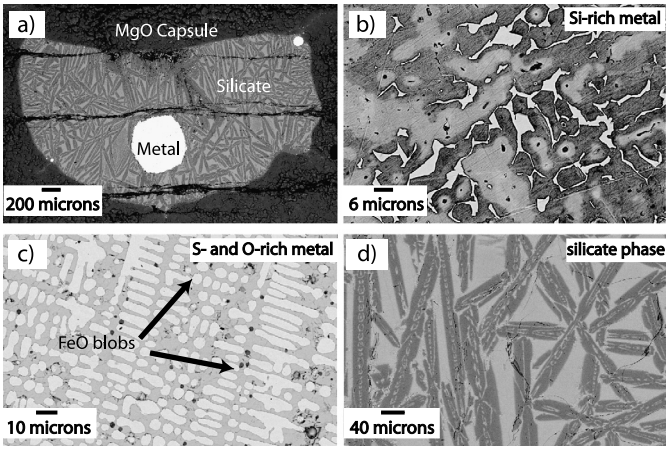

Fig. 1. Images are from samples equilibrated at 2 GPa and 2073 K. a) Backscattered electron image of a typical recovered run (here MORB FeSi95). b) Metallic quench texture on MORB FeSi-90. c) Metallic quench texture of MORB FeS9. d) Typical silicate quenches textures with olivine crystals surrounded by pyroxenite glass (here for MORB FeSi95).

Our starting materials consisted in natural MORB doped at the wt.% level in Ga (2 or 5 wt.%). Consequently, high concentrations of gallium are observed in the metallic and silicate phases of our recovered samples. Nevertheless, previous studies from Drake et al. (1984) and Chabot et al., 2003 showed a conformance to Henry's law across a large Ga concentration, both in the metallic and in the silicate phase. Thus, having samples containing a large amount of Ga will not compromise our capacity to apply our results to core formation scenarios.

Table 2
Pressure, temperature and composition of data from Siebert et al. (2011) used for studying the effect of C on Ga partitioning between metal and silicate.

Run #	50	41	94	116	118	124	126	143	144
T (K)	2123	2123	2173	2123	2173	2123	2123	2123	2123
P (GPa)	1.5	1.5	3	3	3	3	3	3	3
X Fe	0.6094	0.6098	0.6337	0.6565	0.6549	0.6308	0.6433	0.6457	0.6470
X C	0.2625	0.2613	0.2677	0.2641	0.2656	0.2652	0.2639	0.2606	0.2605
X Ga	0.0031	0.0034	0.0041	0.0127	0.0127	0.0092	0.0098	0.0097	0.0097
Log K_D	−0.941	−0.941	−0.945	−1.01	−1.03	−0.916	−0.805	−0.86	−0.932

As the present experiments were performed at a single pressure and only two temperatures, the discussion focuses primarily on the influence of the light elements on Ga partitioning. Also, as the influence of carbon was not specifically considered here, results of Siebert et al. (2011) are included in subsequent discussion and parameterizations to provide a more complete analysis of the influence of the most likely light elements in the Earth's core (Table 2).

Experiments carried out with only silicon in the metallic phase show a clear effect of this element on gallium partitioning. Increase of silicon content in the metallic phase decreases systematically the metal–silicate partitioning of Ga by more than an order of magnitude over the range of composition (up to 16wt.% of Si in the (Fe, Si alloy)).

A previous experimental work of Chabot et al. (2010) focused on the effect of silicon on the partitioning of various trace elements (Ga, Au, Pt, ...) between two metallic liquids in the ternary (Fe, Si, S) system. In their experiments, they demonstrated strong silicon avoidance for gallium in qualitative agreement with our results. Adding silicon to the metallic phase resulted in lowering redox conditions in the samples by reducing FeO from the silicate according to:

$$Si^{metal} + 2FeO^{silicate} \rightarrow SiO_2^{silicate} + 2Fe^{metal} \quad (11)$$

This is not problematic for determining gallium partitioning, as we are using $\log K_D$ that intrinsically normalizes by the quantity of FeO.

As the only parameter that changes from one run to another is the quantity of silicon in the metallic phase, thermodynamic interaction parameter of silicon has been calculated (see Section 6). Our data are coherent with data from the literature (Mann et al., 2009) when corrected for gallium valence.

As presented in Fig. 3, runs containing sulfur (at 2073 K) resulted in enhanced incorporation of oxygen, as indicated by the presence of FeO-rich phases in the quenched metal, and is consistent with previous results (Hillgren and Boehler, 1998; Chabot and Agee, 2003). To separate the effect of these elements on gallium partitioning, we performed experiments at lower temperature (1673 K) and same pressure (2 GPa) to reduce oxygen incorporation in the metallic phase. Decreasing the temperature of our experiments does not have an important effect on gallium partitioning, as temperature does not affect gallium partitioning (Mann et al., 2009; Righter et al., 2010; Siebert et al., 2011).

It is clear from our experiment that both sulfur and oxygen influence gallium partitioning. Indeed, in our low-temperature runs containing negligible oxygen, the value of $\log K_D$ is always higher than that determined at 2073 K when higher concentrations of oxygen are present. We first determine the value of ε^S_{Ga} thanks to our experiments HP-BT1-5 containing no oxygen in the metallic phase, then corrected from this effect the value of $\log K_D$ calculated for experiments MORB FeS 1-14 and MORB FeSSi 5-11.

Table 3
Literature data used to performed multi regression in order to determine the values of a, b and c (Siebert et al., 2011 (a) and Mann et al., 2009 (b)).

Data	T (K)	P (GPa)	Log K_D	Source
52	2123	1.5	−0.028	(a)
139	2123	3	−0.045	(a)
140	2123	3	−0.225	(a)
141	2123	2	−0.278	(a)
142	2123	1	−0.193	(a)
145	2123	0.5	−0.001	(a)
MA17	2173	10	−0.557	(a)
MA18	2123	10	−0.447	(a)
MA20	2123	5	−0.246	(a)
MA21	2123	15	−0.529	(a)
MA22	2173	18	−0.732	(a)
CDF1-3	2023	2	−0.232	(b)
CDF1-4	2023	2	−0.251	(b)
Z457	2473	18	−0.760	(b)

6. Thermodynamic parameterization

The thermodynamic formalism developed above (equation (7)) has been employed to evaluate values of interaction parameters. K_D values for each experiment are measured with the electron microprobe (EPMA). Parameters a, b and c are obtained by least-squares multivariate linear regression using data from Mann et al. (2009) and Siebert et al. (2011) devoid of light elements (Table 3) and performed with MgO capsule. Mann et al. (2009) used a valence of 2+ for Ga in the silicate melt unlike most of other studies (e.g. (Drake et al., 1984; Capobianco et al., 1999; Jaeger and Drake, 2000; Righter and Drake, 2000; Righter et al., 2010; Schmitt et al., 1989; Righter, 2011)). As valence is used to calculate K_D, we recalculated all K_D's values derived by Mann et al. (2009) with a valence of 3+ to consistently calculate a, b and c value.

We find that the temperature term b is not statistically significant ($b = 954 \pm 2982$), as has been noted previously (Mann et al., 2009; Siebert et al., 2011). We finally obtain:

$$\log K = -0.08(0.07) - 79(8)\frac{P}{T} \quad (12)$$

Values in bracket are 1-sigma uncertainties on the parameters.

We used a rearranged version of equation (7) to determine values of interaction parameters (ε^S_{Ga}, ε^{Si}_{Ga}, ε^O_{Ga} and ε^C_{Ga}) so that:

$$\log K - \log K_D = \log \frac{\gamma^{metal}_{Ga}}{(\gamma^{metal}_{Fe})^{3/2}} \quad (13)$$

We evaluated values of epsilon that best fit our experimental dataset and used tabulated values of ε^S_S (−5.65), ε^S_O (−17.08), ε^C_C (12.81) and ε^{Si}_{Si} (12.4) from the Steelmaking Data Sourcebook and ε^O_O (−1) from Tsuno et al. (2013). We considered $\gamma^O_{Ga} = 1$ as there is no data on the activity coefficient of Ga in pure molten iron, and $\varepsilon^{Ga}_{Ga} = 0$ also because of the scarcity of measurements. This approximation is valid given the similar value of K_D derived from

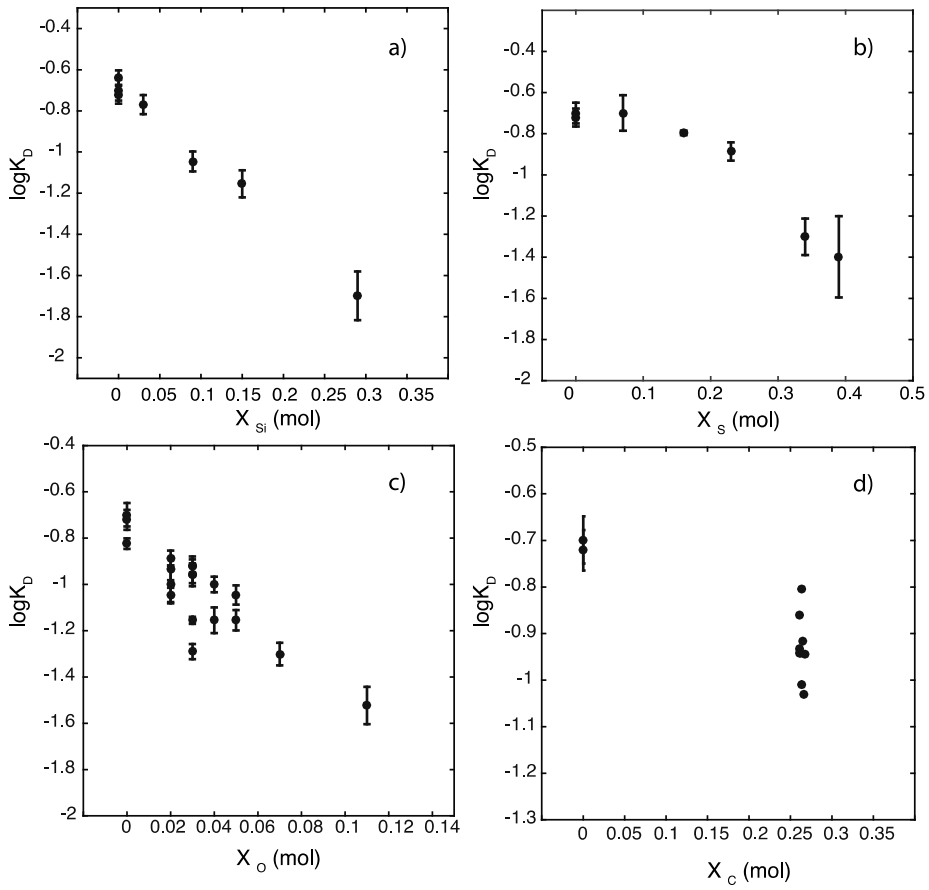

Fig. 2. Effect of light elements on gallium partitioning at 2 GPa, 2073 K for (a) and (c); 2 GPa, 1673 K for (b) and 1–3 GPa and 2123–2123 K for (d) (see Tables 1 and 2). Errors are smaller than the symbol size when not visible.

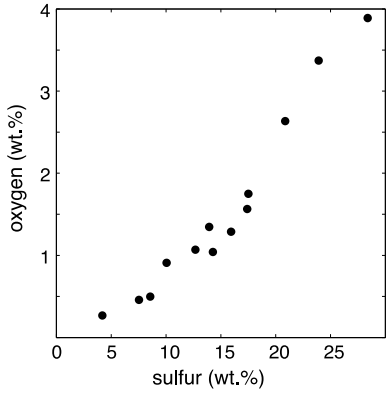

Fig. 3. Oxygen versus sulfur content of the metallic melt measured at EPMA for runs performed at 2073 K and 2 GPa with Fe + FeS as starting material. This graph highlights the increasing incorporation of oxygen in the metallic phase linked to the augmentation of sulfur content of the starting material.

our experiments containing no light elements in the metallic phase but various amount of Ga (6 and 2.5 wt.%, see Fig. 2).

We obtained the following interaction parameters, normalized to the metallurgy standard temperature of 1873 K using equation (10), with their associated uncertainties in brackets:

ε^{S}_{Ga} (1873 K) = 5.35 (0.38)

ε^{Si}_{Ga} (1873 K) = 9.98 (2.15)

ε^{O}_{Ga} (1873 K) = 17.9 (2.6)

ε^{C}_{Ga} (1873 K) = 5.6 (0.2)

estimated the value ε^{S}_{Ga} with our S-rich low temperature experiments (2 GPa–1673 K) and then integrated it to equation (13) to determine ε^{O}_{Ga}.

The value derived for ε^{S}_{Ga} is lower, but agree in sign, than the one determined recently by Wood et al. (2014) ($\varepsilon^{S}_{Ga} = 6.54$). However, this study did not take into account interaction of different elements amongst themselves, and especially the effect of oxygen on sulfur (ε^{S}_{O}) for their calculation of γ^{metal}_{Fe}. This can be a source of error for the estimate of ε^{S}_{Ga} as sulfur and oxygen strongly interact with each other in liquid metal ($\varepsilon^{S}_{O} = -17.08$ Steelmaking Data Sourcebook, 1988).

The large effect of oxygen observed on Ga partitioning disagrees with the work of Chabot et al. (2014) where Ga partitioning is poorly affected by the presence of O in the metallic phase. Nevertheless, in their study they investigate Ga partitioning between two immiscible metallic liquids instead of metal–silicate partitioning as we performed in this study.

7. Core formation models

The adequacy of a core formation model is typically assessed by its success in predicting the partitioning of a particular element between the bulk silicate Earth and the core. Gallium concentration in the bulk silicate Earth is 4 ppm (O'Neill and Palme, 1998). An estimate of the quantity of gallium in the Earth's core can be obtained via mass balance assuming a chondritic bulk Earth. CI chondrites contains 9.8 ppm gallium, EH chondrites 16.7 ppm and ordinary chondrites contain on average 6 ppm Ga (Lodders and Fegley, 1998).

The mass balance for gallium on Earth, is given as:

$$Ga_{BE} = 0.68 * Ga_{BSE} + 0.32 * Ga_{core}$$

with BSE for Bulk Silicate Earth and BE for Bulk Earth where 0.68 and 0.32 the respective mass fractions of the mantle and core in the bulk Earth.

Normalizing the abundance of gallium in chondrites (either carbonaceous or EH) we obtain:

$$\frac{Ga_{BE}}{Ga_{chondrite}} = 0.68 * \frac{Ga_{BSE}}{Ga_{chondrite}} + 0.32 * \frac{Ga_{core}}{Ga_{chondrite}}$$

Sodium and gallium have about the same 50% condensation temperature at 10^{-4} bar (958 and 980 K respectively, Lodders, 2003), but sodium is strictly lithophile. Thus, one can write:

$$\frac{Ga_{BE}}{Ga_{chondrite}} = \frac{Na_{BE}}{Na_{chondrite}} = 0.68 * \frac{Na_{BSE}}{Na_{chondrite}}$$

$$\frac{Ga_{core}}{Ga_{chondrite}} = \frac{0.68}{0.32} * \left[\frac{Na_{BSE}}{Na_{chondrite}} - \frac{Ga_{BSE}}{Ga_{chondrite}} \right]$$

From this equation, knowing that the Bulk Silicate Earth contains 2670 ppm Na, CI chondrites contain 5000 ppm and EH chondrites 6880 ppm (and ordinary chondrites are intermediate, Lodders and Fegley, 1998; McDonough and Sun, 1995), we can estimate the abundance of gallium in the core. For a CI-like Earth, we predict a core containing 2.4 ± 1.9 ppm of Ga; and for a EH-like Earth, a core containing 5.3 ± 2.3 ppm of Ga. We also calculated the bulk composition of the Earth in Ga depending on which chondrite is considered and taking into account volatility effect. For a CI-like Earth, we estimated a Ga content of 3.5 ± 0.7 ppm and 4.4 ± 0.8 ppm for an EH-like Earth.

We can then calculate the resulting D_{Ga} ($= X_{Ga}^{core}/X_{Ga}^{BSE}$) from Eq. (3): assuming a CI chondrite Earth leads to $D_{Ga} = 0.6$ (± 0.5), while an EH chondrite Earth results in $D_{Ga} = 1.3$ (± 0.6). Those two values include uncertainties on the composition of BE in Ga and Na, along with their respective abundances uncertainties in meteorites (CI and EH). Following McDonough and Sun (1995), we estimated that the uncertainties associated with the abundance of gallium on the BSE as 10%, and for chondrite 5%. The core–mantle concentration ratio is the effective global partition coefficient, and constitutes the geochemical target used to assess our models.

Core formation was modeled as a succession of events occurring while the Earth accretes, where molten metal segregates and equilibrates at the base of a magma ocean. In this scenario, the P–T conditions at the base of the magma ocean evolve as the Earth grows (Wade and Wood, 2005). The Earth is accreted in 1% mass steps and the core-to-mantle mass ratio remained fixed at all steps and equal to the present-day value of 0.47 (Wade and Wood, 2005; Ricolleau et al., 2011; Siebert et al., 2012, 2013). At each step, metal and silicate equilibrate at the base of the magma ocean, and then the metal is removed to the core. Our thermodynamic model is used to estimate the partitioning of gallium between the core and silicate melt at each step in the core formation model, calculating D_{Ga} for different final pressures of equilibration and different redox paths.

Models include final magma ocean pressures from 30 GPa to 70 GPa. Pressure at the base of the magma ocean evolves as the Earth grows and pressure at each step i is given by:

$$P(i) = P_{final} * M(i)^{2/3}$$

with P_{final} the final pressure at the base of the magma ocean and $M(i)$ the accreted mass fraction at step i.

To be consistent with the magma ocean hypothesis, the temperature at its base must lie between the mantle solidus and liquidus.

For the first modeling presented in this paper (Fig. 4), two different geotherms were used: a warm liquidus from Fiquet et al. (2010), and a cool liquidus from the average of Fiquet et al. (2010) and Andrault et al. (2011).

In the literature, tremendous efforts have been carried out to better constraints the conditions under which differentiation of the Earth occurred in terms of redox conditions. Two scenarios are in direct opposition: the reduced versus the oxidized scenario. In the first one (especially support by works of Wade and Wood, 2005; Wood et al., 2006 and Rubie et al., 2011), Earth accretion is proposed to have taken place from highly reduced to more oxidized conditions toward the end. On the contrary, the second one (supported by Righter and Ghiorso, 2012 and Siebert et al., 2013) suggests that the building blocks of the Earth evolved from oxidized to reduced during the course of accretion. For now, the debate on the redox conditions during Earth accretion is still ongoing. Nevertheless, in the past decades, the first scenario has received more attention in the literature.

To better constrain the redox history during accretion/core formation four different fO_2 paths and their effect on gallium partitioning are considered. In this study, we fixed an a priori FeO evolution during core formation and the FeO content in the mantle varied linearly throughout accretion. The final FeO content of the mantle is always fixed to the present-day value of 8 wt.%. Model A considers reduced conditions (initial FeO is 0.8 wt.%), Model B a constant redox scenario (8 wt.% FeO), Model C and D are for oxidizing conditions with initial FeO at 11 wt.% and 24 wt.%, respectively. As stated earlier in the text, there is yet no consensus on which redox scenario occurred during Earth differentiation, thus we explore here a wide range of magma ocean redox to best test all hypothesis. In the following, the pressure range of core formation has been calculated based on nickel and cobalt metal–silicate partitioning experiments from the literature; and is represented Fig. 4 as the light grey area.

The uncertainties on all thermodynamic parameters (a, c, ε_{Ga}^{Si}, ε_{Ga}^{S}, ε_{Ga}^{O} and ε_{Ga}^{C}) were propagated to obtain D_{Ga}, using Monte Carlo simulation. We calculated 10^5 samples of D_{Ga} randomly sampling the thermodynamic parameters from normal distributions with the means and standard errors associated with each parameter. The average and standard deviation on the randomly sampled D_{Ga} were calculated to obtain the mean value and the 1-sigma uncertainty on D_{Ga} (Fig. 4).

To assess the influence of light elements on gallium partitioning, two independent sets of calculation were performed: one where the metal was constrained to be pure Fe, and another where the amount of silicon and oxygen were calculated self-consistently from metal–silicate phase equilibration using published thermodynamic models (Siebert et al., 2013). The values of D_{Ga} for a pure Fe core (i.e. without light elements) do not reproduce the target Earth value regardless of pressure, redox, or temperature (Fig. 4, dashed line).

Including silicon and oxygen in the metallic phase result in lowering the value of D_{Ga} whatever the redox path that is considered. Nevertheless, the terrestrial target defined previously is only achieved in the case of very oxidizing condition (Fig. 4D with FeO varying from 24 to 8 wt.% in the mantle) and at high pressure ($P > 50$ GPa).

Finally, we consider the influence of carbon and sulfur. Following Dasgupta et al. (2013), the amount of carbon that can enter the core is fixed at a maximum value of 0.2 wt.%. We also consider a core containing 2 wt.% sulfur, the maximum suggested by Dreibus and Palme (1996). Addition of both carbon and sulfur results in lower values of D_{Ga}, for a fixed concentration of Si and O. This implies that a C- and S-bearing core would require less Si and O to match gallium concentrations in the mantle, at a fixed magma ocean depth. Alternatively, adding C and S to the core at constant Si and O concentration would satisfy mantle gallium concentration in a shallower magma ocean. At any rate, the effect of S and C,

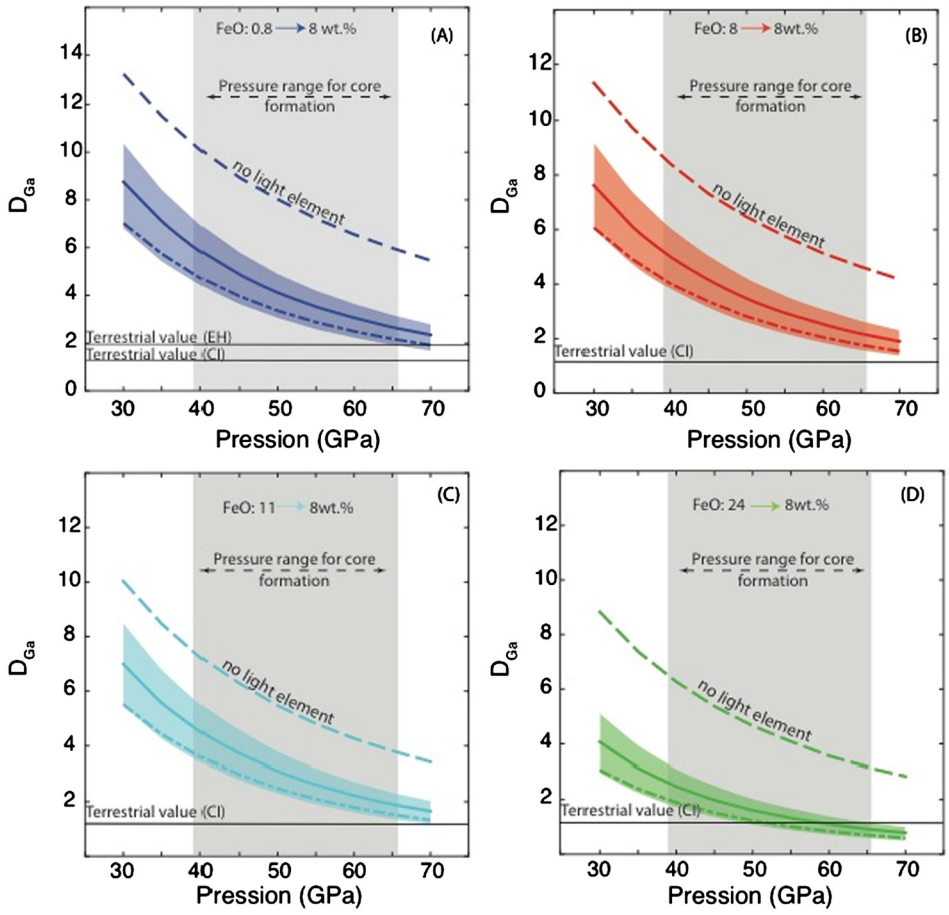

Fig. 4. The final D_{Ga} after continuous core formation as a function of magma ocean final pressure (i.e. depth) for different redox conditions. The four quadrats correspond to four redox paths during accretion. Dark blue (A) is for reduced conditions (from initial FeO at 0.8 wt.%), red (B) is for a constant FeO equal to present, blue (C) is for oxidizing conditions starting at 11 wt.% and green (D) is a more oxidizing path with initial FeO at 24 wt.%. Final FeO is always fixed to the present-day value of 8 wt.% and the evolution is linear between initial and final. O and Si in the core are calculated self-consistently. The curve labeled as "no light elements" stands for a continuous core formation model in which no light element is incorporated in the growing core. The full line stands for the mean between the warm and the cool liquidus (Fiquet et al., 2010 and Andrault et al., 2011), the shaded area stands for the uncertainty associated with the mean. The dotted line is the mean calculated for a core containing an additional 2 wt.% S and 0.2 wt.% C. The line labeled as "Terrestrial value" is the upper bond of the estimate D_{Ga} on Earth, taking into account uncertainties on the concentration of Ga and Na in bulk Earth and in meteorites (either CI or EH). (For interpretation of the references to color in this figure legend, the reader is referred to the web version of this article.)

when their concentration in the core is limited to generally accepted cosmochemical and geophysical limits, does not drastically change the conclusion that Si and O are required in the core.

To account for gallium metal–silicate partitioning, our models require a deep magma ocean, with a final pressure of at least 50 GPa together with oxidizing conditions. This pressure is coherent with what has been proposed in the literature for the last pressure of equilibration (Wade and Wood, 2005; Siebert et al., 2013; Walter and Trønnes, 2004; Bouhifd and Jephcoat, 2011; Siebert et al., 2012).

To further quantify the effect of light elements on gallium partitioning, we calculated the light-element concentration thresholds where D_{Ga} falls in the terrestrial target calculated above (i.e. $D_{Ga} = 0.6$ (± 0.5) for CI chondrites and $D_{Ga} = 1.3$ (± 0.6) for EH chondrites). Here, the Si and O concentrations were not calculated from experimentally determined partition coefficients, but rather fixed from the start, hence becoming additional input parameters to the model. A systematic investigation was undertaken where the quantity of oxygen and silicon in the core was varied independently from 0 to 20 wt.% for silicon and 0 to 12 wt.% for oxygen by 1% steps, generating a square O–Si composition grid of 1024 possibilities. The continuous core formation models were run for each of these compositions, at different magma ocean depths, redox and with and without additional 2 wt.% sulfur and 0.2 wt.% carbon in the core (Dreibus and Palme, 1996; Dasgupta et al., 2013). We used the average of two geotherms proposed in the literature in our calculations to compute the temperature at each pressure stage (Fiquet et al., 2010 and Andrault et al., 2011).

For the sake of clarity, the O and Si thresholds for which D_{Ga} satisfies the terrestrial mantle observable are presented at a single pressure of 50 GPa in Fig. 5. This high pressure is coherent with the one derived from our previous modeling (Fig. 4).

The colored area defines the frontier between allowed and non-allowed D_{Ga} domains, i.e. area where a certain combination of Si and O with or without S and C can account for terrestrial D_{Ga}. The upper limit represents solutions where no S and C were added, whereas the lower one stands for the S- and C-rich core (respectively 2 and 0.2 wt.%).

Under highly reducing conditions (Fig. 5A with FeO content of the mantle ranging from 0.8 to 8 wt.% during the course of accretion) such as those found in enstatite chondrites (around IW-4), silicon is the main light element in the core. In this case, very high silicon concentrations (>12 wt.%) are needed to satisfy the gallium partitioning constraints. Such high concentrations are difficult to reconcile with the seismological observed density deficit in the core. Combined seismological and mineral-physics constraints on inner-core composition limit the maximum silicon

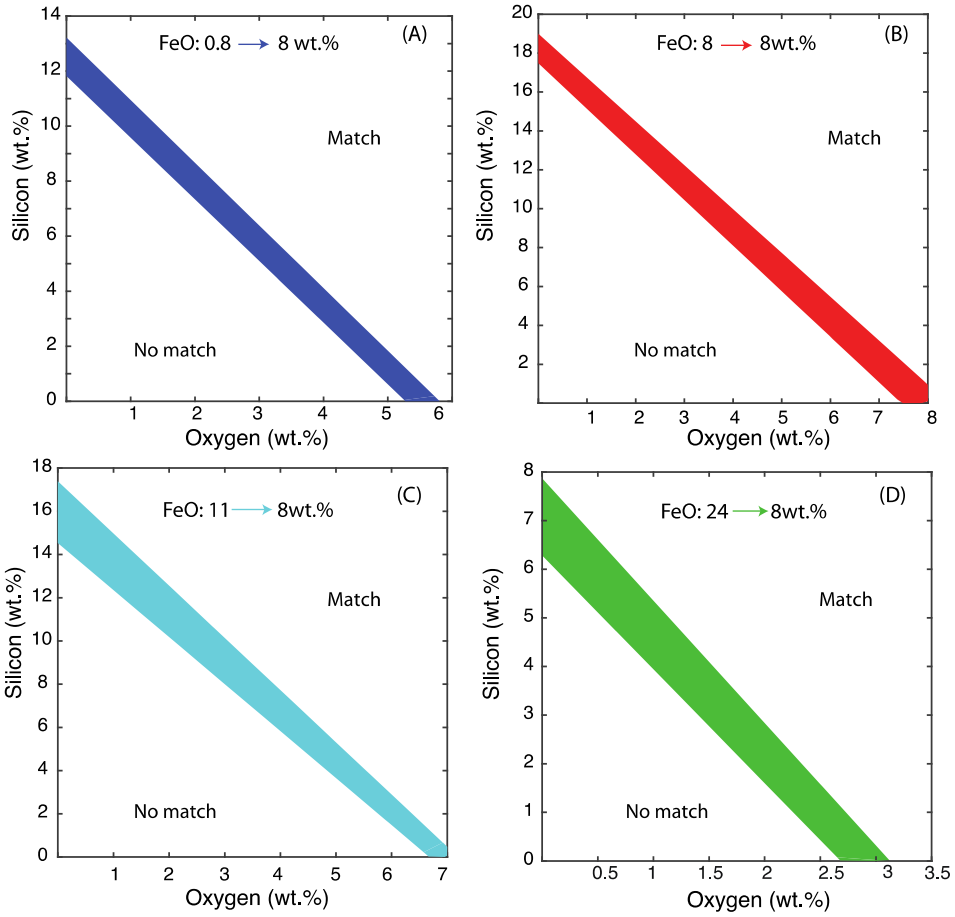

Fig. 5. Delimitation of O–Si contents in the core for which D_{Ga} ($0 < D_{Ga} < 1.9$ for model A and $0 < D_{Ga} < 1.07$ for models B, C, D) satisfies the terrestrial mantle observable. The higher O and Si, the closer D_{Ga} is to the target value. The two domains (matching and non-matching composition) are separated by the colored area, corresponding to no S and C in the core for its upper bond, and for an additional 2 wt.% S and 0.2 wt.% C in the core for its lower bond. The four quadrats correspond to four redox paths during accretion. Dark blue (A) is for reduced conditions (from initial FeO at 0.8 wt.%), red (B) is for a constant FeO equal to present, blue (C) is for oxidizing conditions starting at 11 wt.% and green (D) is a more oxidizing path with initial FeO at 24 wt.%. Final FeO is always fixed to the present-day value of 8 wt.% and the evolution is linear between initial and final. The temperature at the base of the magma ocean is fixed to the mean of the two geotherm proposed by Fiquet et al. (2010) and Andrault et al. (2011). (For interpretation of the references to color in this figure legend, the reader is referred to the web version of this article.)

concentrations in the core to 2–3.5 wt.% (Antonangeli et al., 2010; Badro et al., 2007). First principles calculations (Badro et al., 2014) of outer-core composition have proposed that the core can contain no more than 4.5 wt.% silicon. In the case of an EH-chondrite Earth, this would require a minimum of 3.5 wt.% oxygen (Fig. 5A) to satisfy the Ga constraint. Incorporating that much oxygen in such reducing conditions is inconsistent with experimental observations (Ricolleau et al., 2011; Tsuno et al., 2013; Siebert et al., 2013). Relaxing that constraint and allowing up to 8 wt.% Si in the core would still require 2 wt.% oxygen, a value inconsistent with experimental observation.

Homogeneous accretion at constant redox also requires unrealistic quantity of oxygen and silicon to be dissolved in the metallic core (Fig. 5B). Indeed, assuming again a core containing 4.5 wt.% of silicon would result in an incorporation of at least 6 wt.% of oxygen, which is above geophysical estimates (Badro et al., 2014).

In the case of slightly oxidizing conditions (Fig. 5C, with FeO content of the mantle varying from 11 to 8 wt.%), a high quantity of light element is also needed. As can be read in Fig. 5C, with 8 wt.% of silicon entering the core, an additional 3 wt.% of oxygen would still be required to account for gallium metal–silicate partitioning. As discussed earlier, such a high quantity of light elements in the core is not coherent either with experimental constrains nor *ab initio* calculation (Tsuno et al., 2013; Siebert et al., 2013; Badro et al., 2014).

Accretion under more oxidizing condition elegantly solves this conundrum (Fig. 5D). Assuming the core can contain no more than 4.5 wt.% Si (Badro et al., 2014), highly oxidized accretion requires about 1 wt.% oxygen in the core. Supposing the core contains less silicon, for example 2 wt.% as suggested by Antonangeli et al. (2010), which is coherent with scenario of oxidizing conditions, would imply a reasonable quantity of oxygen to be dissolved in the metallic phase (i.e. about 2 wt.%). Those content of silicon and oxygen are well within the range of what has been proposed in the literature from metal–silicate partitioning experiments (Takafuji et al., 2005) and *ab initio* calculation (Badro et al., 2014).

Thus, this model is consistent with the Si and O concentrations in a metal in equilibrium with a silicate at high FeO content (about 20 wt.%). Therefore, the only way to explain the high Ga concentrations in the Bulk Silicate Earth along with O and Si concentrations that satisfy experimental observation, is to segregate the core in a deep magma ocean that is more oxidizing than the present-day mantle, as has been proposed on the basis of the depletion of other siderophile elements (Siebert et al., 2013). We point out that experimental results of this study come from piston–cylinder experiments and do not cover the full range of extreme P and T conditions of core formation process. Systematic study of Ga partitioning at higher pressure and temperature using the diamond anvil cell technique and laser heating is required to validate models presented here.

8. Conclusion

We have shown from metal–silicate partitioning experiments that gallium concentrations in the mantle can be reconciled with core formation scenarios if the core contains light elements, solving a long-standing conundrum. Our models show that core–mantle equilibrium must have occurred at minimum pressure of 50 GPa, strengthening the hypothesis of a deep magma ocean (Li and Agee, 1996) during Earth differentiation. Models where the core contains no light elements fail to reproduce gallium concentration in the mantle. On the other hand, varying amounts of silicon and oxygen yield satisfactory models only in the case of oxidizing conditions. This conclusion is independent of sulfur and carbon concentrations up to maximum suggested values of 2 and 0.2 wt.% in the core, respectively. The silicon content at low redox often falls above the acceptable valued for the present-day core, and violates the observations from radial seismological models (Badro et al., 2014). The silicon and oxygen concentrations at low, to medium redox are not sufficient to obtain a final gallium concentration compatible with mantle observables, even if equilibrium took place at very high pressure. Conversely, highly oxidizing conditions (magma ocean FeO concentration >19 wt.%) yielding higher amounts of Si and O in the core allow the matching of mantle concentration at high pressures of equilibration. Therefore, our conclusions strongly favor oxidizing conditions during core formation. Direct experiments at high pressure (40–70 GPa) are under way in the laser-heated diamond anvil cell to confirm this trend.

Acknowledgements

The research leading to these results has received funding from the European Research Council under the European Community's Seventh Framework Programme (FP7/2007-2013)/ERC grant agreement No. 207467. We acknowledge the financial support of the UnivEarthS Labex Program at Sorbonne Paris Cité (ANR-10-LABX-0023 and ANR-11-IDEX-0005-02). J.S. acknowledges financial support from the PNP research program from INSU and the French National Research Agency (ANR project VolTerre, grant no. ANR-14-CE33-0017-01). We thank Kevin Righter and an anonymous reviewer for comments that led to an improved and clarified paper.

Appendix A. Supplementary material

Supplementary material related to this article can be found online at http://dx.doi.org/10.1016/j.epsl.2015.06.063.

References

Andrault, D., Bolfan-Casanova, N., Nigro, G.L., Bouhifd, M.A., Garbarino, G., Mezouar, M., 2011. Solidus and liquidus profiles of chondritic mantle: implication for melting of the Earth across its history. Earth Planet. Sci. Lett. 174, 181–191.

Antonangeli, D., Siebert, J., Badro, J., Farber, D.L., Fiquet, G., Morard, G., Ryerson, F.J., 2010. Composition of the Earth's inner core from high-pressure sound velocity measurements in Fe–Ni–Si alloys. Earth Planet. Sci. Lett. 295, 292–296.

Badro, J., Fiquet, G., Guyot, F., Gregoryanz, E., Occelli, F., Antonangeli, D., d'Astuto, M., 2007. Effect of light elements on the sound velocities in solid iron: implications for the composition of Earth's core. Earth Planet. Sci. Lett. 254, 233–238.

Badro, J., Côté, A.S., Brodholt, J.P., 2014. A seismologically consistent compositional model of Earth's core. Proc. Natl. Acad. Sci. USA 132.

Birch, F., 1952. Elasticity and constitution of the Earth's interior. J. Geophys. Res. 57, 227–286.

Birch, F., 1964. Density and composition of mantle and core. J. Geophys. Res. 69, 4377–4388.

Bouhifd, M.A., Jephcoat, A.P., 2011. Convergence of Ni and Co metal–silicate partition coefficients in the deep magma–ocean and coupled silicon–oxygen solubility in iron melts at high pressures. Earth Planet. Sci. Lett. 307, 341–348.

Brenan, J.M., McDonough, W.F., 2009. Core formation and metal–silicate fractionation of osmium and iridium from gold. Nat. Geosci. 2, 798–801.

Capobianco, C.J., Drake, M.J., de Aro, J., 1999. Siderophile geochemistry of Ga, Ge, and Sn: cationic oxidation states in silicate melts and the effect of composition in iron–nickel alloys. Geochim. Cosmochim. Acta 63, 2667–2677.

Chabot, N.L., Agee, C.B., 2003. Core formation in the Earth and Moon: new experimental constraints from V, Cr, and Mn. Geochim. Cosmochim. Acta 67, 2077–2091.

Chabot, N.L., Campbell, A.J., Jones, J.H., Humayun, M., Agee, C.B., 2003. An experimental test of Henry's law in solid metal–liquid metal systems with implications for iron meteorites. Meteorit. Planet. Sci. 38, 181–196.

Chabot, N.L., Draper, D.S., Agee, C.B., 2005. Conditions of core formation in the Earth: constraints from nickel and cobalt partitioning. Geochim. Cosmochim. Acta 69, 2141–2151.

Chabot, N.L., Safko, T.M., McDonough, W.F., 2010. Effect of silicon on trace element partitioning in iron-bearing metallic melts. Meteorit. Planet. Sci. 45 (8), 1243–1257.

Chabot, N.L., Alex Wollack, E., Humayun, M., Shank, E.M., 2014. The effect of oxygen as a light element in metallic liquids on partitioning behavior. Meteorit. Planet. Sci.

Corgne, A., Keshav, S., Wood, B.J., McDonough, W.F., Yingwei, F., 2008. Metal-silicate partitioning and constraints on core composition and oxygen fugacity during Earth accretion. Geochim. Cosmochim. Acta 72, 574–589.

Corgne, A., Siebert, J., Badro, J., 2009. Oxygen as a light element: a solution to single-stage core formation. Earth Planet. Sci. Lett. 288, 108–114.

Cottrell, E., Walter, M.J., Walker, D., 2009. Metal–silicate partitioning of tungsten at high pressure and temperature: implications for equilibrium core formation in Earth. Earth Planet. Sci. Lett. 281, 275–287.

Dasgupta, R., Chi, H., Shimizu, N., Buono, A.S., Walker, D., 2013. Carbon solution and partitioning between metallic and silicate melts in a shallow magma ocean: implications for the origin and distribution of terrestrial carbon. Geochim. Cosmochim. Acta 102, 191–212.

Drake, M.J., Newsom, H.E., Reed, .S.J.B., Enright, M.C., 1984. Experimental determinationof the partitioning of gallium between solid iron metal and synthetic basaltic melt: electron and ion microprobe study. Geochim. Cosmochim. Acta 48, 1609–1615.

Dreibus, G., Palme, H., 1996. Cosmochemical constraints on the sulfur content in the Earth's core. Geochim. Cosmochim. Acta 60, 1125–1130.

Ertel, W., O'Neill, H.S.C., Dingwell, D., Spettel, B., 1996. Solubility of tungsten in a haplobasaltic melt as a function of temperature and oxygen fugacity. Geochim. Cosmochim. Acta 60, 1171–1180.

Fiquet, G., Auzende, A.L., Siebert, J., Corgne, A., Bureau, H., Ozawa, H., Garbarino, G., 2010. Melting of peridotite to 140 gigapascals. Science 329, 1516–1518.

Gessmann, C.K., Rubie, D.C., 1998. The effect of temperature on the partitioning of nickel, cobalt, manganese, chromium, and vanadium at 9 GPa and constraints on formation of the Earth's core. Geochim. Cosmochim. Acta 62 (5), 867–882.

Gessmann, C.K., Rubie, D.C., 2000. The origin of the depletions of V, Cr and Mn in the mantles of the Earth and Moon. Earth Planet. Sci. Lett. 184, 95–107.

Gessmann, C.K., Wood, B.J., Rubie, D.C., Kilburn, M.R., 2001. Solubility of silicon in liquid metal at high pressure: implications for the composition of the Earth's core. Earth Planet. Sci. Lett. 184 (2), 367–376.

Hillgren, V.J., Boehler, R., 1998. High pressure reactions between metals and silicates: implications for the light element in the core and core–mantle. Mineral. Mag. 62A, 624–625.

Holzheid, A., Sylvester, P., O'Neill, H.S.C., Rubie, D., Palme, H., 2000. Evidence for a late chondritic veneer in the Earth's mantle from high-pressure partitioning of palladium and platinum. Nature 406, 396–399.

Jaeger, W.L., Drake, M.J., 2000. Metal-silicate partitioning of Co, Ga, and W: dependence on silicate melt composition. Geochim. Cosmochim. Acta 64, 3887–3895.

Li, J., Agee, C.B., 1996. Geochemistry of mantle–core differentiation at high pressure. Nature 381, 686–689.

Lodders, K., 2003. Solar system abundances and condensation temperatures of the elements. Astrophys. J. 591 (2), 1220.

Lodders, K., Fegley, B., 1998. The Planetary Scientist's Companion. Oxford Univ. Press.

Ma, Z., 2001. Thermodynamic description for concentrated metallic solutions using interaction parameters. Metall. Mater. Trans., B Process Metall. Mater. Proc. Sci. 32 (1), 87–103.

Mann, U., Frost, D.J., Rubie, D.C., 2009. Evidence for high-pressure core–mantle differentiation from the metal–silicate partitioning of lithophile and weakly-siderophile elements. Geochim. Cosmochim. Acta 73, 7360–7386.

McDonough, W.F., 2003. Compositional model for the Earth's core. In: Treatise on Geochemistry, vol. 2, pp. 547–568.

McDonough, W.F., Sun, S.-S., 1995. The composition of the Earth. Chem. Geol. 120 (3), 223–253.

O'Neill, H.S.C, Palme, H., 1998. Composition of the silicate Earth: implications for accretion and core formation. In: The Earth's Mantle: Composition, Structure and Evolution, vol. 1.

O'Neill, H.S.C., Canil, D., Rubie, D.C., 1998. Oxide-metal equilibria to 2500° C and 25 GPa: implications for core formation and the light component in the Earth's core. J. Geophys. Res., Solid Earth (1978–2012) 103 (B6), 12239–12260.

Palme, H., O'Neill, H.S.C., 2003. Cosmochemical estimates of mantle composition. In: Treatise on Geochemistry, vol. 2, pp. 1–38.
Ricolleau, A., Fei, Y., Corgne, A., Siebert, J., Badro, J., 2011. Oxygen and silicon contents of Earth's core from high pressure metal–silicate partitioning experiments. Earth Planet. Sci. Lett. 310, 409–421.
Righter, K., 2011. Prediction of metal–silicate partition coefficients for siderophile elements: an update and assessment of PT conditions for metal–silicate equilibrium during accretion of the Earth. Earth Planet. Sci. Lett., 158–167.
Righter, K., Drake, M.J., 2000. Metal/silicate equilibrium in the early Earth–new constraints from the volatile moderately siderophile elements Ga, Cu, P, and Sn. Geochim. Cosmochim. Acta 64, 3581–3597.
Righter, K., Ghiorso, M.S., 2012. Redox systematics of a magma ocean with variable pressure-temperature gradients and composition. Proc. Natl. Acad. Sci. USA 109 (30), 11955–11960.
Righter, K., Drake, M.J., Yaxley, G., 1997. Prediction of siderophile element metal–silicate partition coefficients to 20 GPa and 2800 °C: the effects of pressure, temperature, oxygen fugacity, and silicate and metallic melt compositions. Phys. Earth Planet. Inter. 100, 115–134.
Righter, K., Pando, K.M., Danielson, L., Lee, C.-T.-A., 2010. Partitioning of Mo, P and other siderophile elements (Cu, Ga, Sn, Ni, Co, Cr, Mn, V, and W) between metal and silicate melt as a function of temperature and silicate melt composition. Earth Planet. Sci. Lett. 291, 1–9.
Ringwood, A.E., 1966. Chemical evolution of the terrestrial planets. Geochim. Cosmochim. Acta 30, 41–104.
Rubie, D.C., Frost, D.J., Mann, U., Asahara, Y., Nimmo, F., Tsuno, K., Kegler, P., Holzheid, A., Palme, H., 2011. Heterogeneous accretion, composition and core–mantle differentiation of the Earth. Earth Planet. Sci. Lett. 301, 31–42.
Schmitt, W., Palme, H., Wänke, H., 1989. Experimental determination of metal/silicate partition coefficients for P, Co, Ni, Cu, Ga, Ge, Mo and W and some implications for the early evolution of the Earth. Geochim. Cosmochim. Acta 53, 173–185.
Scott, E.R.D., Wasson, J.T., 1975. Classification and properties of iron meteorites. Rev. Geophys. 13, 527–546.
Siebert, J., Corgne, A., Ryerson, F.J., 2011. Systematics of metal–silicate partitioning for many siderophile elements applied to Earth's core formation. Geochim. Cosmochim. Acta 75, 1451–1489.
Siebert, J., Badro, J., Antonangeli, D., Ryerson, F.J., 2012. Metal-silicate partitioning of Ni and Co in a deep magma ocean. Earth Planet. Sci. Lett., 189–197.
Siebert, J., Badro, J., Antonangeli, D., Ryerson, F.J., 2013. Terrestrial accretion under oxidizing conditions. Science.
The Japan Society for the Promotion of Science and The Nineteenth Committee on Steelmaking, 1988. Part 2: recommended values of activity and activity coefficients, and interaction parameters of elements in iron alloys. In: Steelmaking Data Sourcebook. Gordon and Breach Science Publishers, New York, pp. 273–297.
Takafuji, N., Hirose, K., Mitome, M., Bando, Y., 2005. Solubilities of O and Si in liquid iron in equilibrium with (Mg, Fe) SiO_3 perovskite and the light elements in the core. Geophys. Res. Lett. 32 (6).
Thibault, Y., Walter, M.J., 1995. The influence of pressure and temperature on the metal–silicate partition coefficients of nickel and cobalt in a model Cl chondrite and implications for metal segregation in a deep magma ocean. Geochim. Cosmochim. Acta 59, 991–1002.
Tsuno, K., Frost, D.J., Rubie, D.C., 2013. Simultaneous partitioning of silicon and oxygen into the Earth's core during early Earth differentiation. Geophys. Res. Lett. 40, 1–6.
Wade, J., Wood, B.J., 2005. Core formation and the oxidation state of the Earth. Earth Planet. Sci. Lett. 236, 78–95.
Walter, M.J., Trønnes, R.G., 2004. Early earth differentiation. Earth Planet. Sci. Lett. 225.
Wood, B.J., Walter, M.J., Wade, J., 2006. Accretion of the Earth and segregation of its core. Nature 441, 825–833.
Wood, B.J., Wade, J., Kilburn, M.R., 2009. Core formation and the oxidation state of the Earth: additional constraints from Nb, V and Cr partitioning. Geochim. Cosmochim. Acta 72, 1415–1426.
Wood, B.J., Kiseeva, E.S., Mirolo, F.J., 2014. Accretion and core formation: the effects of sulfur on metal–silicate partition coefficients. Geochim. Cosmochim. Acta.